Improved SST-precipitation intraseasonal relationships in the ECMWF coupled climate reanalysis

Geophysical Research Letters

RESEARCH LETTER
10.1029/2018GL077138

Key Points:
- SST-precipitation intraseasonal relationships are well captured in CERA-20C and misrepresented in its predecessor ERA-20C
- Improved relationships in CERA-20C are due to improved intraseasonal SST through the coupled analysis
- The coupled model of CERA-20C in the 2000s can well simulate SST-precipitation intraseasonal relationships

Supporting Information:
- Supporting Information S1

Correspondence to:
X. Feng,
xiangbo.feng@reading.ac.uk

Citation:
Feng, X., Haines, K., Liu, C., de Boisséson, E., & Polo, I. (2018). Improved SST-precipitation intraseasonal relationships in the ECMWF coupled climate reanalysis. *Geophysical Research Letters*, *45*, 3664–3672. https://doi.org/10.1029/2018GL077138

Received 24 JAN 2018
Accepted 30 MAR 2018
Accepted article online 6 APR 2018
Published online 23 APR 2018

Improved SST-Precipitation Intraseasonal Relationships in the ECMWF Coupled Climate Reanalysis

Xiangbo Feng[1], Keith Haines[1,2], Chunlei Liu[1,2], Eric de Boisséson[3], and Irene Polo[1]

[1]Department of Meteorology, University of Reading, Reading, UK, [2]National Centre for Earth Observation, University of Reading, Reading, UK, [3]European Centre for Medium-Range Weather Forecasts, Reading, UK

Abstract The European Centre for Medium-range Weather Forecasts (ECMWF) has produced the ocean-atmosphere coupled reanalysis for the twentieth century, CERA-20C, following on from the similar but atmosphere-only reanalysis ERA-20C. Here we demonstrate the capability of CERA-20C in producing more physically consistent ocean and atmosphere boundary conditions, by focusing on sea surface temperature (SST)-precipitation intraseasonal relationships. CERA-20C reproduces well the observed SST-precipitation correlations, while these relationships are poorly represented in ERA-20C, with the greatest discrepancies in the early 1900s. The improved relationships in CERA-20C are due to intraseasonal improvements in SST that are not present in the external HadISST2 product. In CERA-20C, SST-precipitation relationships are slightly weaker in the 1900s than in the 2000s, mainly due to differences in the assimilated observation density. We also find that the coupled model initialized from CERA-20C in the 2000s realistically simulates these relationships, while relaxing SST toward HadISST2 tends to damp these relationships. CERA-20C has improved mean and variance in precipitation over ERA-20C, but these are mostly due to improvements in the atmospheric model and not due to coupled feedbacks.

Plain Language Summary Climate reanalyses, reconstructions of past weather and climate conditions, are of importance in the climate research and forecasting community. The European Centre for Medium-range Weather Forecasts has recently launched its first ocean-atmosphere coupled reanalysis for the twentieth century, known as CERA-20C. Many users are expected. One of the main breakthroughs of this state-of-the-art data set is resolving the air-sea interactions via coupled modeling, while the ocean and atmosphere models are constrained separately by observations. This paper shows that the sea surface temperature-precipitation relationships are much better reproduced in CERA-20C than in its predecessors. Such significant improvement in CERA-20C is due to the ocean surface that more realistically reflects the intraseasonal variations in the atmosphere through the coupled processes. The results highlight the advances of coupled reanalysis in producing physically consistent ocean and atmosphere conditions, indicating that we are moving in the right direction on climate reanalysis. This could have an immediate impact on the plans for producing global climate reanalyses at some institutions. In addition, the metrics of lead-lag correlations applied here could be easily implemented to other climate data sets, to evaluate the quality of climate data.

1. Introduction

Climate reanalyses for past climate are mainly based on atmospheric general circulation models, which are constrained by observations through data assimilation (DA). Such uncoupled (atmosphere-only) reanalyses will have a specified evolving sea surface temperature (SST) based on observational analyses, as far as they are available, as the boundary conditions, along with other forcing terms (e.g., CO_2, aerosols, and ozone) in the atmosphere for long-term records. The National Centers for Environmental Prediction (NCEP) Reanalyses (Kalnay et al., 1996; Kanamitsu et al., 2002), Twentieth Century Reanalysis (Compo et al., 2011), Modern-Era Retrospective analysis for Research and Applications (MERRA; Rienecker et al., 2011), and ERA-Interim (Dee et al., 2011) are examples of such products with varying degrees of refinements on the long-term forcing. One major limitation in uncoupled reanalyses is the lack of atmospheric feedbacks onto the ocean boundary conditions. For producing more consistent ocean-atmosphere reanalyses, coupled general circulation models have recently started to be used in DA, with the most recent examples being the NCEP's Climate Forecast System Reanalysis (CFSR; Saha et al., 2010, 2014), UK Met Office's coupled DA system (Lea et al., 2015) and the Coupled European Centre for Medium-range Weather Forecasts (ECMWF)

ReAnalysis system (CERA; Laloyaux et al., 2016). Such systems are based on coupled models with DA implemented individually for the atmosphere and ocean components and are usually named as "weakly" coupled DA systems as no cross-medium background error covariances are directly used (Lu et al., 2015; Sluka et al., 2016). It is essential to assess the strengths and weaknesses of these coupled reanalyses with respect to uncoupled equivalents, but this can be difficult because coupled reanalyses often have different resolution or use different atmospheric models.

Air-sea interactions at the interface between the ocean and atmosphere are of key importance for the coupled Earth system. The relationship between precipitation and underlying SSTs is an important measure for air-sea interactions on intraseasonal timescales (Arakawa & Kitoh, 2004; Woolnough et al., 2000). Higher SSTs will encourage precipitation both through surface evaporation increasing humidity and vertical atmospheric instability increasing convection, tending to result in positive SST-precipitation correlations with SST leading precipitation (e.g., Kirtman & Vecchi, 2011). Here we will refer to this as "Ocean Forcing." On the other hand, the stronger surface winds and thickening cloud during precipitation events, especially over the tropical oceans, lead to evaporative cooling and reduced downward shortwave radiation (e.g., Fu & Wang, 2004; Woolnough et al., 2000), both tending to reduce the SST after some days of lag. These cooling effects, along with smaller impacts from other surface heat fluxes (i.e., sensible heat and longwave fluxes), drive negative SST-precipitation correlations, here referred to as "Atmospheric Forcing." The resultant SST-precipitation correlations are therefore the result of balance between these Ocean and Atmospheric Forcings, as has been demonstrated both in observations and in coupled general circulation models (Arakawa & Kitoh, 2004; Lau & Sui, 1997; Rajendran et al., 2012; Wu & Kirtman, 2005; Wu et al., 2006). In areas with stronger ocean dynamics, such as in the eastern Equatorial Pacific, the Ocean Forcing remains dominant in the SST-precipitation relationships as the SST variability is too large to be significantly modulated by the Atmospheric Forcing.

Kumar et al. (2012) and Saha et al. (2010) compared the SST-precipitation intraseasonal relationships in existing uncoupled reanalyses (ERA-Interim, MERRA, and NCEP Reanalyses R1 and R2) with coupled CFSR reanalysis. Kumar et al. (2012) concluded that the improved relationships in CFSR reanalysis are due to better specifications of SSTs (via strong SST relaxation) but not due to the coupled analysis system. In addition, negative SST-precipitation correlations were found in these uncoupled reanalyses. This may be because in all of these reanalyses (i) SST is prescribed or constrained by high-frequency (daily-to-weekly) SST observations and (ii) the precipitation variability on intraseasonal timescales is largely controlled by the assimilated atmospheric observations, and it remains similar among different reanalyses. SST-atmosphere relationships in these data sets can reflect correlations in the assimilated high-frequency observations themselves.

Following the long atmosphere-only reanalysis ERA-20C (Poli et al., 2016), ECMWF has recently produced its first ocean-atmosphere coupled reanalysis CERA-20C (Feng et al., 2018; Laloyaux et al., 2016). In these two products, SST is either prescribed or relaxed toward a low-frequency (monthly) SST product HadISST2 (Titchner & Rayner, 2014). However, in CERA-20C the SST intraseasonal variability is largely a result of interactions between the ocean and atmosphere systems and is not strongly constrained by the SST relaxation (this will be addressed in section 2), with the SST relaxation playing the dominant role in the SST longer-term variability (Feng et al., 2018). Therefore, comparing SST-precipitation relationships between ERA-20C and CERA-20C, in which differences in model resolution and physics are minimized, will explicitly reveal the advantages of air-sea coupling in climate reanalysis.

CERA-20C, with its advanced coupled DA scheme, is a state-of-the-art long-term climate reanalysis (Buizza et al., 2017), and many users are expected in the climate research and forecasting communities. It is important to examine the merit of this data set in relation to its predecessors, and here we demonstrate the capability of CERA-20C to produce the SST-precipitation intraseasonal relationships. The roles of DA and model coupling in producing such relationships are also investigated.

2. Data and Methodology

ERA-20C is the ECMWF atmosphere-only reanalysis for the twentieth century based on the Integrated Forecasting System (IFS, version cy38r1) with the resolution set to T159/L91 (Poli et al., 2016). CERA-20C, known as the ECMWF atmosphere-ocean coupled climate reanalysis for the twentieth century (Buizza et al., 2017; Feng et al., 2018), is based on CERA (Laloyaux et al., 2016), in which DA is applied individually for the

atmosphere and ocean components. CERA-20C uses the IFS as ERA-20C, but it is an updated IFS version (cy41r2). In CERA-20C, the IFS is coupled with the Nucleus for European Modelling of the Ocean model (NEMO, version 3.4) at frequency of 1 hr, using the ORCA1 ocean grid, with 42 vertical levels with a top layer thickness of 10 m. CERA-20C also has 10 ensemble members generated by perturbing observations and model physical tendencies (Feng et al., 2018). In this paper, we show results from the control member of CERA-20C. The analysis using the ensemble mean or different ensemble members of CERA-20C does not alter the results.

In these two reanalyses, the IFS assimilates the same observations of surface pressure and marine wind from the International Comprehensive Ocean-Atmosphere Data Set (ICOADS; Woodruff et al., 2011) and the International Surface Pressure Databank (ISPD; Compo et al., 2010; Cram et al., 2015) using the 4DVAR scheme with a 24-hr assimilation window. In CERA-20C, NEMO assimilates the observational profiles of subsurface ocean temperature and salinity from EN4.02 (Good et al., 2013) using the 3DVAR scheme (Mogensen et al., 2012) with the same assimilation window as the atmosphere.

In ERA-20C, SST is prescribed by the daily version of the monthly observation-based HadISST2 (Titchner & Rayner, 2014). Daily SST fields are obtained by temporal interpolation of monthly fields from adjacent months (Hersbach et al., 2005). There is no temporal variability less than 30 days other than the interpolated changes explicitly produced in the daily version of HadISST2. In CERA-20C, the temperature of the top layer of NEMO is relaxed toward the daily version of HadISST2 via a relaxation scheme developed in ORAS4 (Balmaseda et al., 2013), to avoid model drift while enabling the simulation of coupled processes. The SST is also indirectly altered by the model iterations applied in CERA. We find that the analyzed SST closely follows HadISST2 at low frequencies ($>$ 60 days; Figure S1b in the supporting information), but on timescales $<$60 days the SST is substantially altered from HadISST2 (Figure S1a). Thus, in CERA-20C the SST intraseasonal (10–60 days) variability is produced substantially by atmosphere-ocean feedback processes within the coupled analysis system.

Unassimilated model runs of ERA-20C and CERA-20C are also used to understand the roles of DA in producing the SST-precipitation relationships. ERA-20CM is the free IFS integration (see Hersbach et al., 2005), with the same model version and configurations as in ERA-20C, with 10 ensemble members. We analyzed the control member of ERA-20CM over 1906–1910 as the "ERA-free" uncoupled model run. A free coupled model run was started from the control member of CERA-20C in 2000, without DA or SST relaxation, for 10 years. To identify the impact of SST relaxation alone, this coupled model was run again but with SST relaxed toward HadISST2. The last 5 years of data were then analyzed as "CERA-free" and "CERA-freeS" runs, respectively.

Daily fields of total precipitation (TP), large-scale precipitation (LSP), convective precipitation (CP), and SST, with 1° × 1° spatial resolution, are used in this paper. In the IFS, TP is the sum of LSP and CP, which are produced by the cloud and convection schemes, respectively (Bechtold et al., 2014; ECMWF, 2016; Forbes et al., 2011). We use the total cloud cover (TCC, %) and vertical motion of air at 800 mbar (W, Pa/s) as proxies for LSP- and CP-related processes in the IFS, as suggested by Watson et al. (2015). Observed TP and SST are obtained from daily 0.25° × 0.25° Tropical Rainfall Measuring Mission (TRMM; Huffman et al., 2010) and Optimum Interpolation Sea Surface Temperature (OISST; Banzon et al., 2016) data sets and then interpolated to a 1° × 1° grid. High-latitude regions ($>$50°S/N) are excluded from the analysis.

Intraseasonal variability is produced by applying a 10- to 60-day band-pass filter to the daily time series at each grid point after removing the seasonal climatology (e.g., Kumar et al., 2012; Saha et al., 2010). Removing the higher-frequency ($<$ 10 days) signals allows the lead-lag correlations to be dominated by the intraseasonal variability. Linear correlation between two variables is then calculated. The significance of the correlation is assessed at the 95% confidence level based on a *t* test. The periods focused on are 2006–2010 (2000s) and 1906–1910 (1900s) when assimilated observations have the highest and lowest availability, respectively.

3. Results

3.1. Reanalyses in the 2000s

Simultaneous SST-TP intraseasonal correlations in observations are shown in Figure 1a. A significant negative correlation ($r = -0.1$ to -0.3) is seen in the precipitating regions, particularly in the Indo-West Pacific, the Intertropical Convergence Zone and the South Pacific Convergence Zone, showing the dominance of

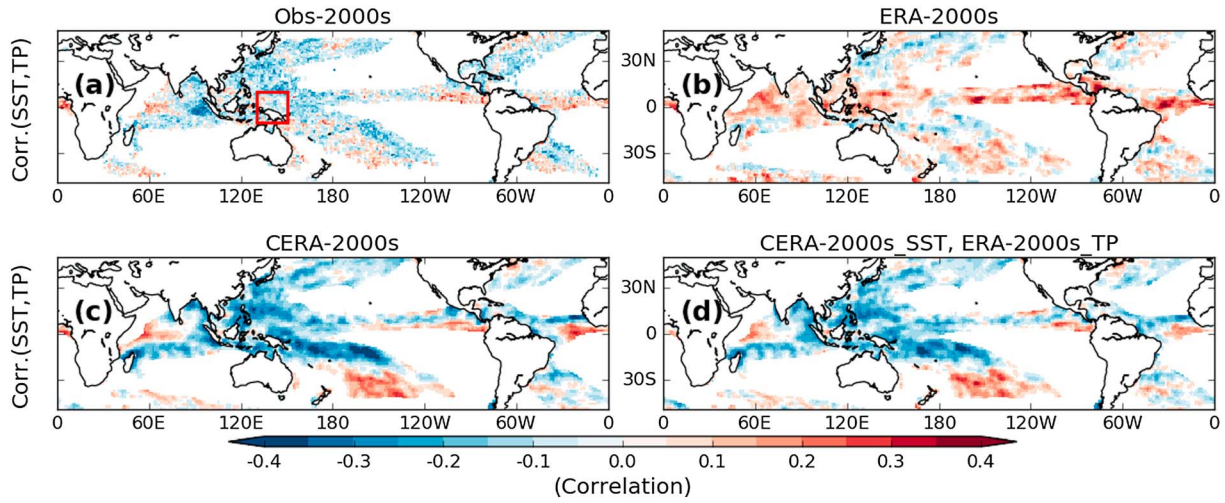

Figure 1. (a–c) Sea surface temperature (SST) and total precipitation (TP) intraseasonal correlations in observations, ERA-20C and CERA-20C, respectively, over 2006–2010. (d) SST and TP intraseasonal correlations with SST from CERA-20C and TP from ERA-20C over 2006–2010. Blank areas are where the correlations do not pass the significance test or where mean TP $<$ 3 mm/day. Red box in (a) shows the area of the tropical western Pacific (10°S–10°N, 130°E–150°E).

Atmospheric Forcing. However, ERA-20C erroneously produces a positive correlation (r = 0.1–0.3) over much of the tropical oceans (Figure 1b), indicating the apparent dominance of Ocean Forcing. In contrast, negative correlations in observations are reproduced in CERA-20C (Figure 1c). When TP anomalies from ERA-20C are correlated with SST anomalies from CERA-20C, the result (Figure 1d) is again negative correlations as in CERA-20C (Figure 1c). This suggests that the improved SST-TP correlations in CERA-20C are mostly due to improved SSTs.

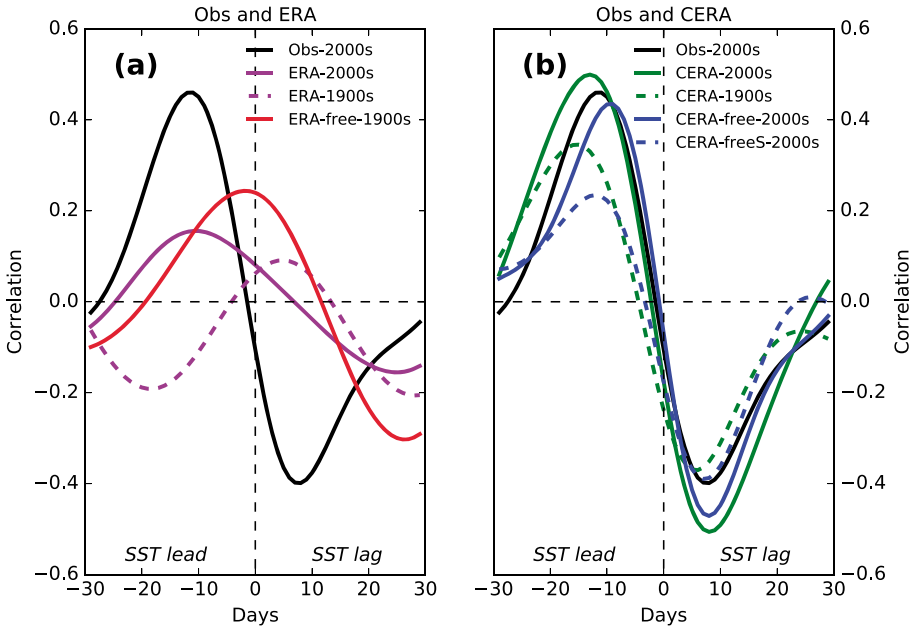

Figure 2. (a) Lead-lag SST and TP intraseasonal correlations in observations over 2006–2010 (black solid line), in ERA-20C over 2006–2010 (magenta solid line) and over 1906–1910 (magenta dashed line), and in ERA-free over 1906–1910 (red solid line), averaged over the tropical western Pacific (10°N–10°S, 130°E–150°E). (b) As in (a) but for correlations in CERA-20C over 2006–2010 (green solid line) and over 1906–1910 (green dashed line) and in CERA-free (blue solid line) and CERA-freeS (blue dashed line) over 2006–2010. SST = sea surface temperature; TP = total precipitation.

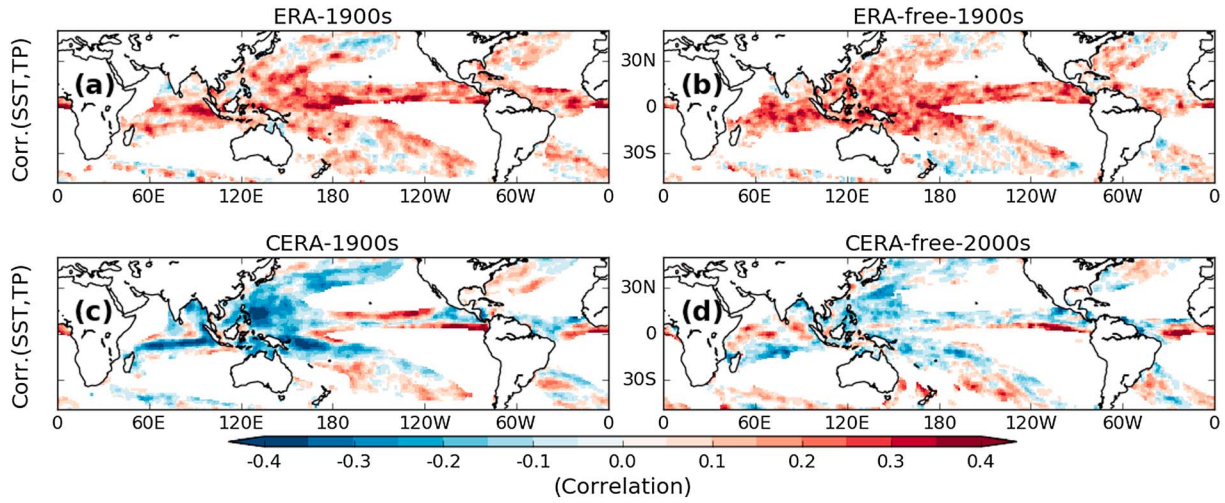

Figure 3. (a, b) SST and TP intraseasonal correlations in ERA-20C and ERA-free over 1906–1910, respectively. (c, d) SST and TP intraseasonal correlations in CERA-20C over 1906–1910 and CERA-free over 2006–2010, respectively. Blank areas are where the correlations do not pass the significance test or where mean TP $<$ 3 mm/day. SST = sea surface temperature; TP = total precipitation.

To further explore the SST-precipitation relationships, lead-lag correlations are calculated for the tropical western Pacific (10°N–10°S, 130°E–150°E; red box in Figure 1a). In observations, positive or negative SST-TP correlation peaks when SST leads or lags TP by ~10 days, respectively (Figure 2), indicating the intraseasonal feedback timescales for Ocean or Atmospheric Forcing. These lead-lag correlations are similar to results in Kumar et al. (2012) using 12 years of data, with our results having slightly larger correlation amplitudes. Figures S2 and S3 show the correlations for the whole precipitating areas, with SST leading or lagging TP by 10 days, respectively.

ERA-20C produces a much weaker relationship in the tropical western Pacific (Figure 2a). The ERA-20C precipitation anomalies are controlled by the large-scale atmospheric variability which is well constrained on intraseasonal timescales by assimilating daily marine surface observations, but the ERA-20C SST, daily interpolated from monthly HadISST2, lacks much of the intraseasonal variability. This inconsistency in timescales means that there is much less chance of showing correlated relationships between the two variables. Also, in Figure 2a we see the positive correlations peak when SST leads TP by ~10 days, the same time as in observations. Much weaker but still negative correlations appear when TP leads SST. These reflect some correlated information existing between the atmospheric observations and HadISST2. The time between peak positive and negative correlations in ERA-20C, ~30 days, then corresponds to the monthly timescale of SST variability resolved in HadISST2.

In the coupled reanalysis CERA-20C, the lead-lag SST-TP correlations in the tropical western Pacific generally agree well with those observed, in terms of both amplitude and phase (Figure 2b). The SST-TP relationships are slightly stronger in CERA-20C than in observations over most of the precipitating regions (Figures 1, 2b, S2, and S3). This may be related to the DA processes in CERA-20C (to be discussed in the next subsection). In short, improved lead-lag correlations are seen in CERA-20C over most precipitating regions.

3.2. Reanalyses in the 1900s, and Free Model Runs

It is important to know how much the DA is contributing to the SST-TP intraseasonal relationships in these two reanalyses, so we take the early years of data and analyze them in the same way. In the early twentieth century, atmospheric observations are rare and provide less constraints on the model. In the 1900s of ERA-20C, the simultaneous SST and TP variability now has an unrealistic positive correlation (r = 0.15–0.4) in precipitating areas (Figure 3a), indicating the apparent dominance of Ocean Forcing. This peaks about 5 days after the SST warming in the tropical western Pacific (Figure 2a). Weak positive lead-lag correlations are also found in these early years for many other regions (Figures S4 and S5). The ERA-free run in the 1900s, without any DA but with SST still prescribed to HadISST2, produces similar SST-TP relationships

as ERA-20C in the 1900s (Figures 3b, S4, and S5), but positive correlations are stronger, such as in the Indo-West Pacific (Figure 2a). In the ERA-free 1900s run, there are no time lags between SST and TP variability, showing the existence of only one-way forcing (Ocean Forcing).

The SST-TP relationships in ERA-20C early years and in ERA-free early years compared with ERA-20C later years show that DA in the atmosphere is generally mitigating the dominance of Ocean Forcing to some degree. In the 1900s, for example, in the tropical western Pacific (Figure 2a), the observational information is limited but is still enough to modify the SST-TP relationships that are established in the free model run, although the resultant relationships still remain substantially biased. However, in the 2000s, more observations provide the reanalysis system with information about atmospheric variability, and consequently, the relationships become more realistic.

In the 1900s of CERA-20C, the spatial distributions of simultaneous SST-TP correlations (Figure 3c) are close to those in the 2000s (Figure 1c), showing the dominance of Atmospheric Forcing on the relationships. The simultaneous correlations are still slightly stronger than observed (Figure 1a). However, the peak amplitudes of the lead-lag correlations are weaker in the 1900s than in the 2000s of CERA-20C and also weaker than in observations (Figures S2, S3, S4, and S5). Figure 2b shows these lead-lag relationships in the tropical western Pacific. Differences in SST-TP relationships between early and later years of CERA-20C mainly indicate the importance of the assimilated observation density.

In the CERA-free 2000s run, the simultaneous SST-TP correlations (Figure 3d) are also close to the observed (Figure 1a) and are even slightly better than in either the 1900s or the 2000s of CERA-20C (Figures 1c and 3c). In the tropical western Pacific, both the amplitude and phase of the lead-lag correlations are also slightly better in the CERA-free 2000s (Figure 2b). This suggests that the coupled model alone simulates well the nonlinear coupling between SST and TP. In the CERA-freeS 2000s run, where SST is relaxed toward HadISST2, the phase of the lead-lag correlations is the same as in CERA-free, but the amplitude is considerably reduced. This shows that the SST relaxation is damping the SST intraseasonal variability in the coupled model and reducing the level of SST-TP coupling. However, when DA is introduced to the atmosphere and ocean in CERA-20C, the SST-TP relationships are strengthened again, at least in the 2000s.

3.3. Relationships With Cloud and Convection

Figure 4a shows the simultaneous SST-LSP correlations in CERA-20C over 2006–2010. SST intraseasonal variability is negatively correlated with LSP in the Indo-West Pacific and western Atlantic, matching closely the SST-TP relationship patterns in Figure 1c. LSP occurs along with cloud spreading and thickening, which reduces SST warming by limiting the solar radiation reaching the ocean surface, resulting in the negative SST-TCC correlations (Figure 4b) and equivalently the positive SST-surface solar radiation correlations (not shown). Cloud has the largest cooling effect on SST when it leads SST by ~10 days in the western tropical Pacific (Figure S6a), agreeing well with the SST-TP relationships in Figure 2b. The SST correlation with TCC in the subtropics is a little more extensive than with LSP, suggesting that cloudiness is strongly related to SST but does not necessarily always lead to precipitation events.

In CERA-20C, the SST intraseasonal variability is also significantly correlated with CP around the Intertropical Convergence Zone and South Pacific Convergence Zone (Figure 4c). Here strong atmospheric convection occurs with fast uplifting of air leading to enhanced surface convergence and enhanced surface winds. The ocean surface is cooled through both increased evaporation and ocean mixing. Therefore, positive SST-W (note $W < 0$ for upward motion) correlations are found wherever the SST-CP correlations are negative (Figure 4d). Negative SST-W correlations appear in the subtropics and the southeastern Pacific and Atlantic, corresponding to regions with subsiding air. In the western tropical Pacific with strong convection, the cooling effect of convection peaks when it leads SST by ~10 days (Figure S6a). We also found that such cooling effects of cloud and convection on SST are stronger in warmer seasons (not shown). This is because SST is more easily cooled when the Atmospheric Forcing is stronger and the ocean mixed layer is shallower.

In contrast, in ERA-20C the SST cannot respond to changes in the atmospheric fields related to cloudiness and precipitation types (Figures 4e–4h and S6b). When repeating the analysis for the early years of data, SST becomes more positively correlated with cloud and convection in the precipitating regions (not shown). This confirms that in ERA-20C precipitation variability is mostly driven by SST, but in the later years this relationship is then modified by the many assimilated atmospheric observations.

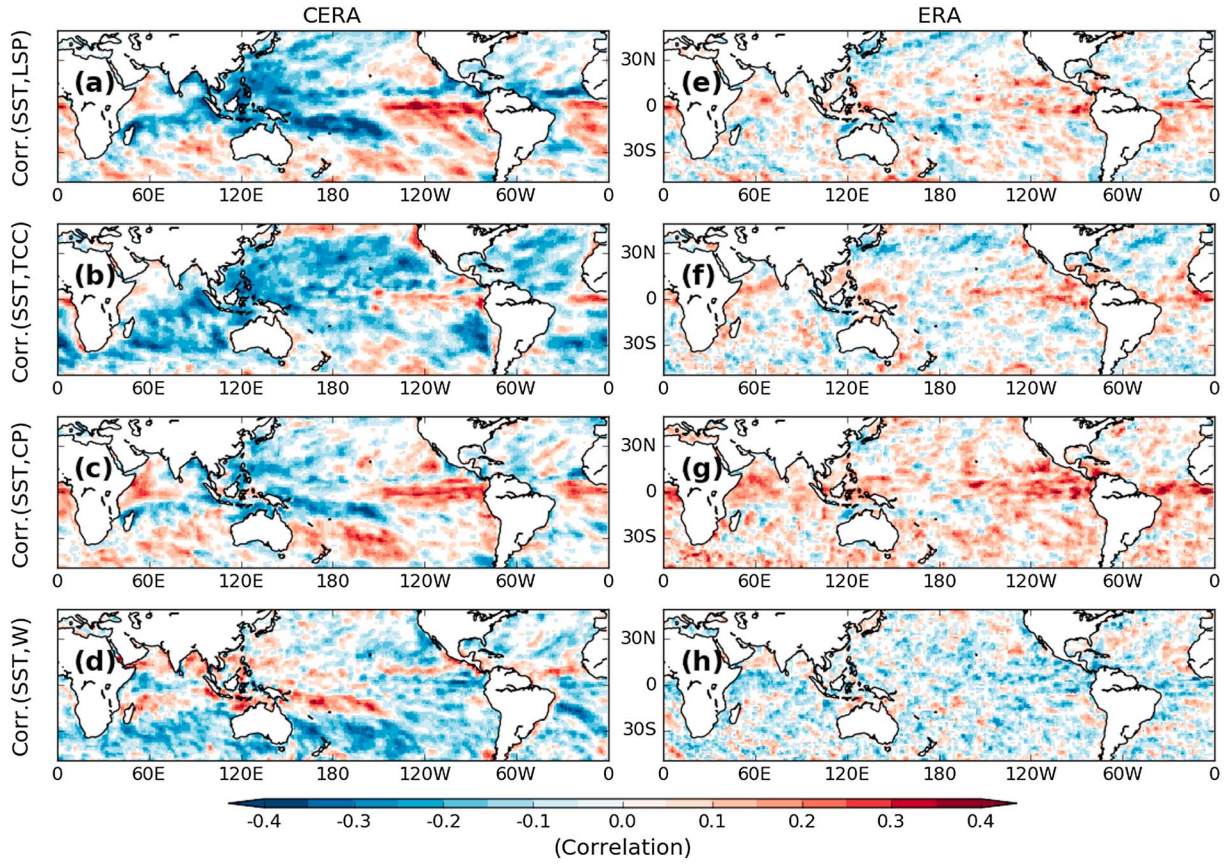

Figure 4. (a–d) SST intraseasonal correlations with large-scale precipitation, total cloud cover, convective precipitation, and vertical motion of air at 800 mbar, respectively, in CERA-20C over 2006–2010. (e–h) As (a–d) but for correlations in ERA-20C over 2006–2010. Note in (d, h) that negative W values mean the air uplift. Blank areas are where the correlations do not pass the significance test. SST = sea surface temperature; LSP = large-scale precipitation; TCC = total cloud cover; CP = convective precipitation; W = vertical motion of air at 800 mbar.

4. Summary and Discussion

In this paper, the SST-precipitation intraseasonal relationships, as an indicator of two-way air-sea coupling, were examined in ECMWF's latest uncoupled and coupled climate reanalyses, ERA-20C and CERA-20C, in which there are only small differences in physics between their atmospheric models. In ERA-20C, the relationships are erroneously represented, due to the lack of atmospheric feedbacks on the ocean. In the 2000s of ERA-20C with many more observations available, these SST-precipitation relationships are improved by assimilating surface observations, but large discrepancies still remain. Better SST-TP relationships in ERA-20C would be obtained for recent years by simultaneously assimilating both atmospheric and SST observations on shorter timescales, as in ERA-Interim (Kumar et al., 2012).

CERA-20C does much better in capturing the observed SST-precipitation relationships, even in the 1900s. However, SST-precipitation relationships are slightly weaker in these early years than in later years of CERA-20C, suggesting the impact of the assimilated observation density. We also found that the coupled NEMO-IFS model of CERA-20C in the later years very realistically simulates the observed SST-precipitation intraseasonal relationships, without any DA or SST relaxation. However, when HadISST2 is used to guide the SST trajectory in the coupled model in the later years, the SST-precipitation relationships are damped. When ocean and atmosphere observations are then assimilated, the timing of intraseasonal SST and precipitation variations is obviously improved and SST-precipitation relationships are strengthened again but become slightly overestimated. This suggests that further adjustment to the coupled DA system may help to further improve the atmosphere-ocean coupling in CERA-20C.

In CERA-20C, the SST-precipitation intraseasonal relationships are a result of air-sea interactions, with the two main contributors to SST cooling being precipitating cloud and convection. The SST-precipitation

relationships also change with seasons and natural climate variability, such as El Niño–Southern Oscillation, as the precipitating regions move around seasonally and interannually. The chemical composition of air, such as aerosols, which induces the formation of clouds and precipitation but is not considered in CERA-20C, may also influence the SST-precipitation relationships.

Comparing ERA-20C and CERA-20C against the TRMM observations over 2006–2010, we find that both reanalyses significantly overestimate the mean precipitation over the oceans by up to 2 mm/day. Over the subtropical oceans the discrepancies of mean precipitation and precipitation intraseasonal variability in CERA-20C are both 0.5–1.0 mm/day smaller than those in ERA-20C. However, ERA-20C and CERA-20C use different versions of the IFS (cy38r1 and cy41r2). Cloud and convection schemes are both changed in the newer version (https://www.ecmwf.int/en/forecasts/documentation-and-support/changes-ecmwf-model). A 1-year (2010) uncoupled reanalysis (as in ERA-20C) using IFS cy41r2 was carried out, and the mean precipitation and precipitation intraseasonal variability amplitudes were found to be very similar to those in CERA-20C. We thus conclude that most of the improvements in time mean and intraseasonal variability of precipitation in CERA-20C are due to the improved atmospheric model and not due to the coupling.

Coupling can strongly modulate the SST variability in the later years of CERA-20C, but it has little impact on the precipitation because the atmospheric circulation and precipitation are strongly constrained by the assimilated atmospheric observations. In the early years of CERA-20C with few observations, coupling could, however, potentially have more of an impact on precipitation, although more modeling work is needed to explore this. This paper demonstrates the capability of CERA-20C to represent dynamically consistent variability between the ocean and atmosphere. It is worth investigating other coupled ocean-atmosphere phenomena in CERA-20C, such as the Madden-Julian Oscillation, in the future. CERA-20C can also be used as initial conditions for coupled forecast models. Compared with separately analyzed ocean and atmospheric initial conditions, CERA-20C should benefit reduced initialization shocks at the start of coupled forecasts (Mulholland et al., 2016), particularly associated with precipitation. Further modeling work is also required to verify this hypothesis.

Acknowledgments

CERA-20C, ERA-20C, and ERA-20CM used in this paper are accessible via the ECMWF public data sets (http://apps.ecmwf.int/datasets/). Free model run data for the 2000s of CERA-20C are available via request to ECMWF data service (dataserv@ecmw.int). Daily 0.25° × 0.25° OISST (V2) data can be accessed via the National Centers for Environmental Information (www.ncdc.noaa.gov/oisst/data-access). Daily 0.25° × 0.25° TRMM (TMPA) Precipitation (L3, V7) can be accessed via the Goddard Earth Sciences Data and Information Services Center (https://pmm.nasa.gov/data-access/downloads). We thank two anonymous reviewers for their helpful comments and suggestions on this work and also thank C. M. Thomas at the University of Reading for reviewing early version of the manuscript. X. F., K. H., and E. B. were supported by the EU FP7 funded ERA-CLIM2 project (607029). C. L. was supported by the NERC funded DEEP-C (K005480/1) and SMURPHS (N006054/1) projects. I. P. was supported by the NERC funded RAMOC (H5193700) and EU FP7 funded PREFACE (603521) projects.

References

Arakawa, O., & Kitoh, A. (2004). Comparison of local precipitation–SST relationship between the observation and a reanalysis dataset. *Geophysical Research Letters*, *31*, L12206. https://doi.org/10.1029/2004GL020283

Balmaseda, M. A., Mogensen, K., & Weaver, A. T. (2013). Evaluation of the ECMWF ocean reanalysis system ORAS4. *Quarterly Journal of the Royal Meteorological Society*, *139*(674), 1132–1161. https://doi.org/10.1002/qj.2063

Banzon, V., Smith, T. M., Chin, T. M., Liu, C., & Hankins, W. (2016). A long-term record of blended satellite and in situ sea-surface temperature for climate monitoring, modeling and environmental studies. *Earth System Science Data*, *8*(1), 165–176. https://doi.org/10.5194/essd-8-165-2016

Bechtold, P., Semane, N., Lopez, P., Chaboureau, J. P., Beljaars, A., & Bormann, N. (2014). Representing equilibrium and nonequilibrium convection in large-scale models. *Journal of the Atmospheric Sciences*, *71*(2), 734–753. https://doi.org/10.1175/JAS-D-13-0163.1

Buizza, R., Brönnimann, S., Haimberger, L., Laloyaux, P., Martin, M. J., Fuentes, M., et al. (2017). The EU-FP7 ERA-CLIM2 project contribution to advancing science and production of Earth-system climate reanalyses. *Bulletin of the American Meteorological Society*. in press. https://doi.org/10.1175/BAMS-D-17-0199.1

Compo, G. P., Whitaker, J. S., Sardeshmukh, P. D., Matsui, N., Allan, R. J., Yin, X., et al. (2011). The twentieth century reanalysis project. *Quarterly Journal of the Royal Meteorological Society*, *137*(654), 1–28. https://doi.org/10.1002/qj.776

Compo, G. P., Whitaker, J. S., Sardeshmukh, P. D., Matsui, N., Allan, R. J., Yin, X., et al. (2010). *International surface pressure databank (ISPDv2)*. Boulder, Colorado, USA: Research Data Archive at the National Center for Atmospheric Research, Computational and Information Systems Laboratory. https://doi.org/10.5065/D6SQ8XDW

Cram, T. A., Compo, G. P., Yin, X., Allan, R. J., McColl, C., Vose, R. S., et al. (2015). The international surface pressure databank version 2. *Geoscience Data Journal*, *2*(1), 31–46. https://doi.org/10.1002/gdj3.25

Dee, D. P., Uppala, S. M., Simmons, A. J., Berrisford, P., Poli, P., Kobayashi, S., et al. (2011). The ERA-Interim reanalysis: Configuration and performance of the data assimilation system. *Quarterly Journal of the Royal Meteorological Society*, *137*(656), 553–597. https://doi.org/10.1002/qj.828

ECMWF (2016). *IFS Documentation CY41R2*. Reading, UK: ECMWF.

Feng, X., Haines, K., & de Boisséson, E. (2018). Coupling of surface air and sea surface temperatures in the CERA-20C reanalysis. *Quarterly Journal of the Royal Meteorological Society*, *144*(710), 195–207. https://doi.org/10.1002/qj.3194

Forbes, R. M., Tompkins, A. M., & Untch, A. (2011). A new prognastic bulk microphysics scheme for the IFS. European centre for medium-range weather forecasts. Technical Memorandum 649. ECMWF: Reading, UK

Fu, X., & Wang, B. (2004). Differences of boreal summer intraseasonal oscillations simulated in an atmosphere–ocean coupled model and an atmosphere-only model. *Journal of Climate*, *17*(6), 1263–1271. https://doi.org/10.1175/1520-0442(2004)017%3C1263:DOBSIO%3E2.0.CO;2

Good, S. A., Martin, M. J., & Rayner, N. A. (2013). EN4: Quality controlled ocean temperature and salinity profiles and monthly objective analyses with uncertainty estimates. *Journal of Geophysical Research: Oceans*, *118*, 6704–6716. https://doi.org/10.1002/2013JC009067

Hersbach, H., Peubey, C., Simmons, A., Berrisford, P., Poli, P., & Dee, D. (2005). ERA-20CM: A twentieth-century atmospheric model ensemble. *Quarterly Journal of the Royal Meteorological Society*, *141*(691), 2350–2375. https://doi.org/10.1002/qj.2528

Huffman, G. J., Adler, R. F., Bolvin, D. T., & Nelkin, E. J. (2010). The TRMM multi-satellite precipitation analysis (TMPA). In F. Hossain, & M. Gebremichael (Eds.), *Chapter 1 in satellite rainfall applications for surface hydrology* (pp. 3–22). Springer Verlag.

Kalnay, E., Kanamitsu, M., Kistler, R., Collins, W., Deaven, D., Gandin, L., et al. (1996). The NCEP/NCAR 40-year reanalysis project. *Bulletin of the American Meteorological Society*, *77*(3), 437–471. https://doi.org/10.1175/1520-0477(1996)077%3C0437:TNYRP%3E2.0.CO;2

Kanamitsu, M., Ebisuzaki, W., Woolen, J., Yang, S. K., Hnilo, J., Fiorino, M., & Potter, G. L. (2002). NCEP–DOE AMIP-II Reanalysis (R-2). *Bulletin of the American Meteorological Society*, *83*(11), 1631–1644. https://doi.org/10.1175/BAMS-83-11-1631

Kirtman, B., & Vecchi, G. A. (2011). *Why climate modelers should worry about atmospheric and oceanic weather* (pp. 511–523). Singapore: World Scientific.

Kumar, A., Zhang, L., & Wang, W. (2012). Sea surface temperature–precipitation relationship in different reanalyses. *Monthly Weather Review*, *141*(3), 1118–1123. https://doi.org/10.1175/MWR-D-12-00214.1

Laloyaux, P., Balmaseda, M., Dee, D., Mogensen, K., & Janssen, P. (2016). A coupled data assimilation system for climate reanalysis. *Quarterly Journal of the Royal Meteorological Society*, *142*(694), 65–78. https://doi.org/10.1002/qj.2629

Lau, K. M., & Sui, C. H. (1997). Mechanisms of short-term sea surface temperature regulation: Observations during TOGA COARE. *Journal of Climate*, *10*(3), 465–472. https://doi.org/10.1175/1520-0442(1997)010%3C0465:MOSTSS%3E2.0.CO;2

Lea, D., Mirouze, I., Martin, M., King, R., Hines, A., Walters, D., & Thurlow, M. (2015). Assessing a new coupled data assimilation system based on the Met Office coupled atmosphere, land, ocean, sea ice model. *Monthly Weather Review*, *143*(11), 4678–4694. https://doi.org/10.1175/MWR-D-15-0174.1

Lu, F., Liu, Z., Zhang, S., & Liu, Y. (2015). Strongly coupled data assimilation using leading averaged coupled covariance (LACC). Part I: Simple model study. *Monthly Weather Review*, *143*(9), 3823–3837. https://doi.org/10.1175/MWR-D-14-00322.1

Mogensen, K. S., Balmaseda, M. A., & Weaver, A. (2012). *The NEMOVAR ocean data assimilation system as implemented in the ECMWF ocean analysis for system 4*, *Technical Memorandum*, (Vol. 668). Reading, UK: ECMWF.

Mulholland, D. P., Haines, K., & Balmaseda, M. A. (2016). Improving seasonal forecasting through tropical ocean bias corrections. *Quarterly Journal of the Royal Meteorological Society*, *142*(700), 2797–2807. https://doi.org/10.1002/qj.2869

Poli, P., Hersbach, H., Dee, D. P., Berrisford, P., Simmons, A. J., Vitart, F., et al. (2016). ERA-20C: An atmospheric reanalysis of the twentieth century. *Journal of Climate*, *29*(11), 4083–4097. https://doi.org/10.1175/JCLI-D-15-0556.1

Rajendran, K., Nanjundiah, R. S., Gadgil, S., & Srinivasan, J. (2012). How good are the simulations of tropical SST–rainfall relationship by IPCC AR4 atmospheric and coupled models? *Journal of Earth System Science*, *121*(3), 595–610. https://doi.org/10.1007/s12040-012-0185-7

Rienecker, M. M., Suarez, M. J., Gelaro, R., Todling, R., Bacmeister, J., Liu, E., et al. (2011). MERRA: NASA's modern-era retrospective analysis for research and applications. *Journal of Climate*, *24*(14), 3624–3648. https://doi.org/10.1175/JCLI-D-11-00015.1

Saha, S., Moorthi, S., Pan, H. L., Wu, X., Wang, J., Nadiga, S., et al. (2010). The NCEP climate forecast system reanalysis. *Bulletin of the American Meteorological Society*, *91*(8), 1015–1058. https://doi.org/10.1175/2010BAMS3001.1

Saha, S., Moorthi, S., Wu, X., Wang, J., Nadiga, S., Tripp, P., et al. (2014). The NCEP climate forecast system version 2. *Journal of Climate*, *27*(6), 2185–2208. https://doi.org/10.1175/JCLI-D-12-00823.1

Sluka, T. C., Penny, S. G., Kalnay, E., & Miyoshi, T. (2016). Assimilating atmospheric observations into the ocean using strongly coupled ensemble data assimilation. *Geophysical Research Letters*, *43*, 752–759. https://doi.org/10.1002/2015GL067238

Titchner, H. A., & Rayner, N. A. (2014). The Met Office Hadley Centre sea ice and sea surface temperature data set, version 2: 1. Sea ice concentrations. *Journal of Geophysical Research: Atmospheres*, *119*, 2864–2889. https://doi.org/10.1002/2013JD020316

Watson, P. A. G., Christensen, H. M., & Palmer, T. N. (2015). Does the ECMWF IFS convection parameterization with stochastic physics correctly reproduce relationships between convection and the large-scale state? *Journal of the Atmospheric Sciences*, *72*(1), 236–242. https://doi.org/10.1175/JAS-D-14-0252.1

Woodruff, S. D., Worley, S. J., Lubker, S. J., Ji, Z., Eric Freeman, J., Berry, D. I., et al. (2011). ICOADS release 2.5: Extensions and enhancements to the surface marine meteorological archive. *International Journal of Climatology*, *31*(7), 951–967. https://doi.org/10.1002/joc.2103

Woolnough, S. J., Slingo, J. M., & Hoskins, B. J. (2000). The relationship between convection and sea surface temperature on intraseasonal timescales. *Journal of Climate*, *13*(12), 2086–2104. https://doi.org/10.1175/1520-0442(2000)013%3C2086:TRBCAS%3E2.0.CO;2

Wu, R., & Kirtman, B. P. (2005). Roles of Indian and Pacific Ocean air–sea coupling in tropical atmospheric variability. *Climate Dynamics*, *25*(2–3), 155–170. https://doi.org/10.1007/s00382-005-0003-x

Wu, R., Kirtman, B. P., & Pegion, K. (2006). Local air–sea relationship in observations and model simulations. *Journal of Climate*, *19*(19), 4914–4932. https://doi.org/10.1175/JCLI3904.1